Quasimolecular x-ray spectrum from 117-keV Ne^{9+} + Ne collisions

M. H. Prior
Chemical Sciences Division, Lawrence Berkeley Laboratory, Berkeley, California 94720

R. Dörner and H. Berg
Institut fur Kernphysik, Universität Frankfurt, D-6000 Frankfurt am Main 90, Germany

H. Schmidt-Böcking,* J. O. K. Pedersen, and C. L. Cocke
J. R. Macdonald Laboratory, Department of Physics, Kansas State University, Manhattan, Kansas 66506-2601
(Received 14 October 1992)

The quasimolecular x-ray spectrum resulting from the filling of a $1s\sigma$ vacancy during the collision of 117-keV Ne^{9+} ions with Ne atoms has been observed in an x-ray ion coincidence experiment for ions scattered into the range 17.0°–26.0°. The observed spectrum is in reasonable agreement with one calculated using the uniform asymptotic approximation and a previous calculation of the $1s\sigma$-$2p\pi$ interval versus the internuclear separation. The model and the data show an interference structure only weakly present due to averaging by the x-ray detector resolution.

PACS number(s): 34.50.Fa

INTRODUCTION

It is well established theoretically [1–5] and experimentally [6–9] that the $1s\sigma$ quasimolecular x-ray emission spectra for swift H-like ions (at fixed impact parameters) show a characteristic interference structure. This oscillating variation of intensity with photon energy yields information on the level spacing of states in the transient quasimolecular collision system. The interference follows from the coherent superposition of nondistinguishable amplitudes for transitions on the incoming half (at collision time $-t_0$) and outgoing half ($+t_0$) of the collision trajectory for the same transition energy. In order to observe interference in the x-ray spectrum a unique (or narrow range of) impact parameters must be selected. This is accomplished by measuring the x-ray spectrum in coincidence with particles scattered at a chosen angle (or narrow range of angles). In addition, the velocity of the H-like ion must be small enough so that the phase differences ($\Delta\phi$) between the interfering amplitudes can exceed π (constructive) or 2π (destructive interference) [7].

Interference structure has been observed in the $1s\sigma$ quasimolecular x-ray emission spectra from collisions of Cl^{16+} on Ar (Refs. [6,7]) and for Kr^{35+} on Mo (Refs. [8,9]). In these works the swift H-like ions were produced by the "acceleration-stripping-deceleration" technique [10–13]. At present this method cannot be applied to much heavier (e.g., Pb^{81+}) or lighter (e.g., Ne^{9+}) ions. Recent improvements in the electron-cyclotron-resonance (ECR) ion sources [14,15], however, make possible similar studies with beams of, e.g., Ne^{9+} or Si^{13+}. The quasimolecular x-ray (QMOX) emission from the Ne^{9+} on the Ne system studied here should give additional interesting information on the orientation of the quasimolecular states during the collision. In this system, the sum occupation number of the $2p\pi$ and $2p\sigma$ states at small internuclear distance should not exceed two. Thus only two transitions can contribute to the $1s\sigma$ radiation which may possibly yield different intensity distributions reflecting the orientation of the quasimolecular orbitals with respect to the scattering plane [16,17].

EXPERIMENTAL METHODS

We have observed the $1s\sigma$ QMOX emission from 117-keV Ne^{9+} collisions with Ne using a photon-particle coincidence set up that is shown schematically in Fig. 1. Ne^{9+} ions were produced by the Lawrence Berkeley Laboratory ECR ion source at the 88-in. cyclotron and transported to the apparatus using the joint LLNL-LBL

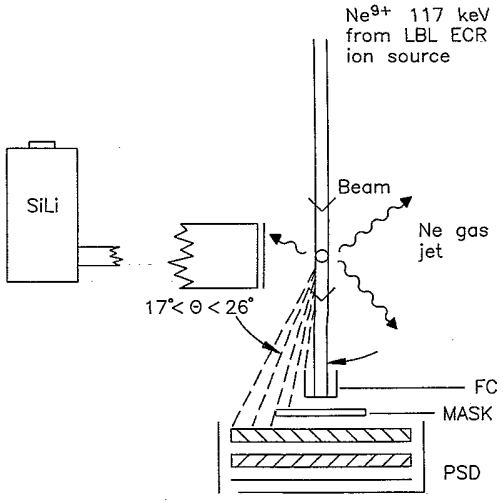

FIG. 1. Schematic of apparatus. ECR denotes an electron-cyclotron-resonance ion source, FC a Faraday cup, and PSD a position-sensitive detector.

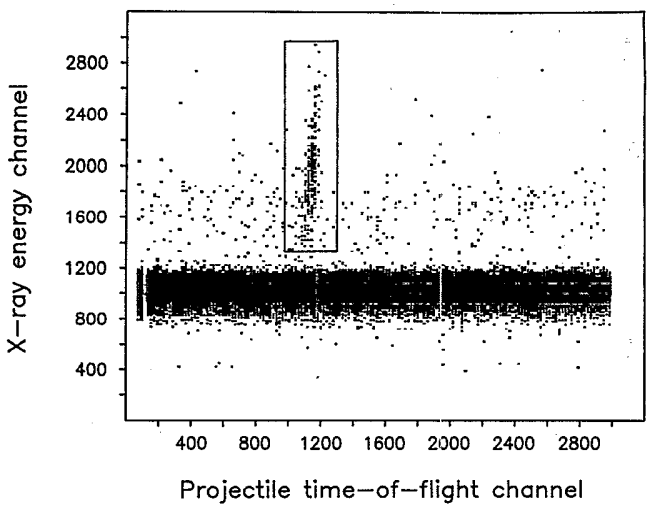

FIG. 2. Density plot of x-ray energy vs projectile flight time. The QMOX events are indicated by the box.

atomic-physics beam-line facilities. Projectiles scattered within the polar scattering range 17°–26° by a Ne gas-jet target struck a two-dimensional position-sensitive detector (PSD). From the position of each projectile on the PSD the azimuthal angle could also be determined. The jet-target region was viewed by a Si(Li) detector placed at 90° to the beam-jet plane. X-ray signals from the Si(Li) detector provided start pulses for a time-to-amplitude (TAC) converter which was stopped by fast pulses from the particle PSD. A data-acquisition computer with mass storage collected and recorded each event (x-ray energy, TAC output, particle position).

Figure 2 is the plot of the x-ray energy versus the projectile time of flight for a portion of the data collected. The preponderance of counts uncorrelated with projectile flight time are accidental coincidences caused by the large flux of Ne K x-ray photons which follow from electron-capture collisions. The rectangular area, outlined in the figure at higher x-ray energies, contains the real QMOX events. The data in this figure are integrated over all scattering angles included by the masked PSD. The projection of this spectrum onto the E_x axis is shown in Fig. 3.

QMOX SPECTRUM

The primary purpose of this experiment was to determine the QMOX spectral shape rather than the absolute emission probability. It was noticed, however, that the measured yield of QMO x rays was much lower than expected on the basis of simple estimates and this rendered the experiment much more difficult than anticipated. During the experiment, approximately 10^{11} scattered particles were detected, for which 4771 coincidences in the QMOX window were registered. When divided by the Si(Li) detector-efficiency–solid-angle factor, this ratio yields a probability of approximately 0.5×10^{-5} per collision that a QMO x ray with energy above 2 keV is emitted. We compare this with a simple estimate based on the quasistatic approximation [5,7]. As described by Schuch *et al.* [7] the approximate yield I of QMO x rays per collision is given by

$$I=2\Gamma_x\Delta R\,(b,E_{\mathrm{xmin}})/v\ ,$$

where E_{xmin} is the lowest x-ray energy for which appreciable emission occurs, v is the collision velocity, Γ_x is the average radiative transition rate and $\Delta R=[R\,(E_{\mathrm{xmin}})^2-b^2]^{1/2}$. We take $E_{\mathrm{xmin}}=2$ keV, from Fig. 3; $b=0.058$ a.u.; $R\,(E_{\mathrm{xmin}})=0.15$ a.u., from Fig. 4. Γ_x can be estimated from dipole scaling of a $2p$ to $1s$ transition, using a matrix element characteristic of a united atom $Z=18$ and a transition energy of 2400 eV. These give a yield I of 0.35×10^{-3} photons per collision, if a single $2p\pi$ electron is available to radiate and the $1s\sigma$ orbital is entirely empty. This rate is about a factor of 70 larger than the observed rate. Even allowing for the possibility that the $1s\sigma$ orbital is only half empty, due to vacancy sharing between $1s\sigma$ and $2p\sigma$ orbitals on the way

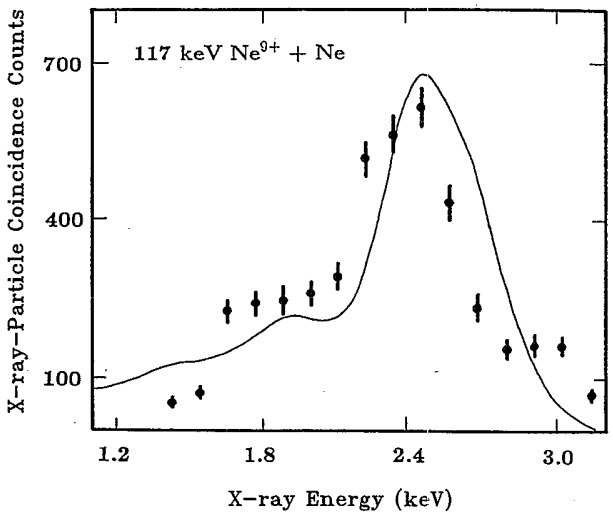

FIG. 3. QMO x-ray spectrum summed over angular range of the experiment.

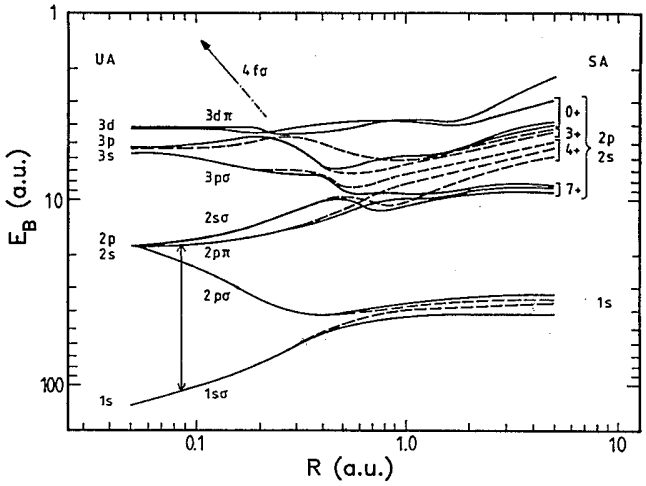

FIG. 4. Molecular orbitals calculated by Wille [20] for Ne^{+9} on Ne.

in, the discrepancy remains large. We attribute this discrepancy to the probable low occupation number for the $2p\pi$ orbital at small R especially for the approach of the collision partners. Referring to the energy-level diagram of Fig. 4, we note that this orbital correlates to large R to the completely empty L shell of the projectile. While some sharing of target L electrons with the projectile L shell is possible on the incoming path, the low collision velocity makes this improbable. No previous QMO x-ray experiments have been carried out at such low v. We note that a similar trend was seen by Schuch *et al.* [7] for Cl^{+16} on Ar, where absolute experimental probabilities were found to lie below calculated ones. That the discrepancy was smaller in that case is presumably due to the higher velocity and greater L sharing for that case. Previous measurements [18,19] have shown that near this collision energy and for these scattering angles, projectile and target final charge states are identical as the result of complete sharing of L electrons; however, this sharing is initially to higher multiply excited states. Relaxations by Auger and radiative processes take place long after the close approach at which QMO x-ray emission occurs.

Figure 3 presents the QMOX energy spectrum integrated over all azimuthal particle scattering angles. The solid line is a computed spectrum which includes the averaging effect of the finite ($\approx$200-eV) x-ray detector resolution. The amplitude of the computed spectrum has been normalized to the data.

The computed spectral shape was calculated following the uniform asymptotic approximation approach as presented by Schuch *et al.* [7], where, for impact parameter b and photon frequency ω, the intensity $I(\omega,b)$ is given by

$$I(\omega,b)=\omega \mathrm{Ai}^2(-x) ,$$

$$x=\left[-\tfrac{3}{2}\phi\right]^{2/3} ,$$

$$\phi=\int_0^{t_b} t\frac{d\omega_{if}(t)}{dt}dt .$$

In the above Ai is the Airy function, $\omega_{if}(t)$ is the energy difference, divided by $\hbar$ between the $2p\pi$ and $1s\sigma$ QMO levels at time t during the collision and t_b is defined by $\omega_{if}(t_b)=\omega$. We have used an approximate formula for $\omega_{if}(R)$, the energy separation of the $2p\pi$ and $1s\sigma$ levels at internuclear separation R, obtained by fitting to the QMO level calculation of Wille [20] (see Fig. 4), that is,

$$\frac{h\omega_{if}}{2\pi}=E_{if}\approx\frac{Ac^2}{R^2+c^2}+B .$$

The constants used were (atomic units) $A=102$, $B=30$, and $c=0.12$. A straight-line trajectory with relative velocity v was used, i.e.,

$$R(t)=[b^2+(vt)^2]^{1/2} ,$$

to provide $\omega_{if}(t)=\omega_{if}(R(t))$. The phase quantity ϕ is then expressible as

$$\phi=\phi_1+\phi_2+\phi_3 ,$$

with

$$\phi_1=\frac{2\pi E_x}{hv}\left[\frac{Ac^2}{E_x-B}-(b^2+c^2)\right]^{1/2} ,$$

$$\phi_2=\frac{-2\pi Ac^2}{hv(b^2+c^2)^{1/2}}\tan^{-1}\left[\frac{vt_b}{(b^2+c^2)^{1/2}}\right] ,$$

and

$$\phi_3=-Bt_b ,$$

where E_x is the photon energy ($\hbar\omega/2\pi$). Finally, assuming a Coulomb scattering of the bare Ne nuclei at 117 keV for the incoming Ne^{9+} ion, one has $[b\ (\text{a.u.})]=0.023/\tan\Theta_{\text{lab}}$, with Θ_{lab} *the laboratory* scattering angle of the projectile. Since Θ_{lab} remains reasonably small, the use of the straight-line trajectory for calculating phase accumulations is not expected to be badly in error.

Figure 5 shows the results of this treatment for three scattering angles, $\Theta_{\text{lab}}=17.0°$, 21.5°, and 26.0° (corresponding to $b=0.075$, 0.058, and 0.047 a.u.) covering the range included in these measurements. Each calculation is weighted by a factor proportional to $\sin\Theta_{\text{lab}}$ to account for azimuthal integration in the particle detector plane. Figure 5 shows that, even for a small impact-parameter range, the oscillatory structure should be effectively washed out by the detector resolution at this beam energy. Thus little is gained by slicing the experimental data into narrow angular bins, and we therefore have chosen to add the data over the entire 17°–26° range for presentation in Fig. 3, since such a sum maximizes the statistical significance of the data. The solid curve in Fig. 3 is

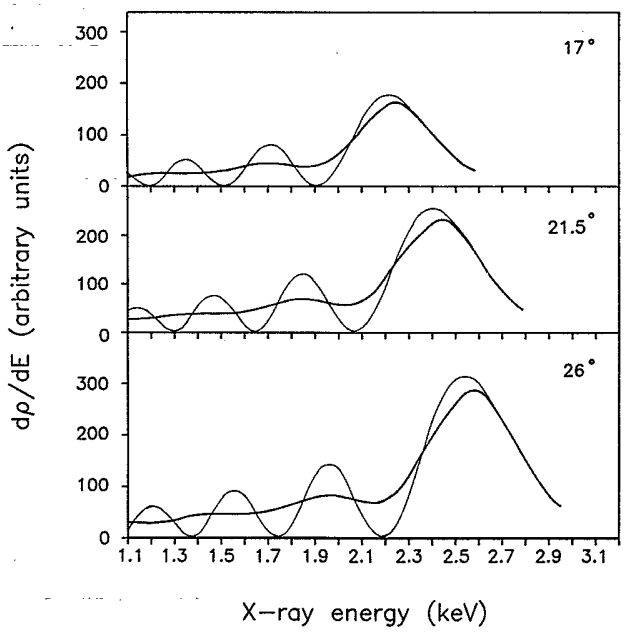

FIG. 5. Model QMO x-ray spectra calculated as described in the text for three representative scattering angles (light lines). The heavy lines show the model results after folding into the Si(Li) detector resolution.

the sum of these three calculations, averaged over the Si(Li) detector resolution of 200 eV.

DISCUSSION

We have observed the QMOX spectra from the filling of a $1s\sigma$ vacancy during the collision of slow (117-keV) Ne^{9+} ions with Ne atoms. The computed spectral shape agrees substantially with the observed one. The strong peak predicted near the stationary phase condition at the distance of closest approach is clearly seen in the data. No oscillation structure is resolved. While previous experiments performed with the acceleration-deceleration technique [6–9] suffered from a slightly too high velocity, such that only one or two oscillations in the pattern could be seen, the present experiment suffers from too low a velocity, such that the oscillation frequency was too high to be resolved at all. This points out the importance of having additional control over the ion velocity from a highly-charged-ion-source facility.

The computed spectral shape, folded into the experimental resolution, is in substantial agreement with the experiment, except that the peak position is not well described. This position is very sensitive to the exact form of the energy difference assumed, and is quite different for transitions to the $1s\sigma$ from $2p\pi$ and $2p\sigma$ initial states. The choice of the $2p\pi$ transition made for the present model calculation was made because that orbital normally gives the larger contribution since the $2p\sigma$ transition rate decreases rapidly as R increases [5]. As mentioned above, on the basis of MO energy levels calculated by Wille [20] for this system (Fig. 4), one expects the $2p\pi$ to correlate to the L shell of the projectile, which is initially empty. Thus QMO radiation on the way into the collision could in this case be due to transitions from the $2p\sigma$ orbital, which correlates to the target K shell and could be fully occupied. However, at small internuclear distances, rotational coupling can move these electrons to the $2p\pi$ orbital, and QMO radiation from this orbital is expected on the outgoing part of the trajectory. A correct calculation of the expected QMO spectrum must take into account the time dependence of the $2p\pi$ and $2p\sigma$ occupation probabilities. In addition, these transitions have very different angular distributions which must be taken into account. For example, the $2p\sigma$ orbital, at the distance of closest approach, will have a dipole transition matrix element which gives no radiation at 90° in the collision plane, while the $2p\pi$ dipole radiation will give maximum radiation of 90°. It is already clear from the disagreement between our simple model and the experiment that the measurement gives sensitive information on both the energy-level structure of the molecular orbitals and the dynamic occupation number in the L shell of the system.

ACKNOWLEDGMENTS

The authors gratefully acknowledge the assistance and hospitality of Drs. C. Lyneis, R. Stokstad, and other members of the LBL 88-in. Cyclotron staff. Particular thanks go to the workshops at LBL, KSU, and U. Frankfort. Important parts of the apparatus were transported from Frankfurt to San Francisco through the generosity of Lufthansa. Support for this work was provided by the Office of Energy Research, Office of Basic Energy Sciences, Chemical Sciences Division, U.S. Department of Energy (H.S.-B., R.D., J.O.K.P., C.L.C.), Kansas State University (H.S.-B., C.L.C.), the Deutsche Forschungsgemeinshaft (H.S.-B., R.D., H.B.), and NATO (J.O.K.P). Additional support was provided by the Friedrich Ebert Stiftung (R.D.) and NATO Research Grant No. 0501/85 (H.B.).

*Present address: Institut fuer Kernphysik, U. Frankfurt, Frankfurt, Germany.

[1] W. Lichten, Phys. Rev. A **9**, 1458 (1974).
[2] J. H. Macek and J. S. Briggs, J. Phys. B **7**, 1312 (1974).
[3] W. Fritsch and U. Wille, J. Phys. B **12**, L335 (1979).
[4] A. Z. Devdariani, U. N. Ostroskii, and A. Niehaus, J. Phys. B **18**, L161 (1985).
[5] R. Anholt, Rev. Mod. Phys. **57**, 995 (1985), and references included.
[6] I. Tserruya, R. Schuch, H. Schmidt-Böcking, J. Barette, Wang Da Hai, B. M. Johnson, K. W. Jones, and M. Meron, Phys. Rev. Lett. **50**, 30 (1983).
[7] R. Schuch, M. Moren, B. M. Johnson, K. W. Jones, R. Hoffman, H. Schmidt-Böcking, and I. Tserruya, Phys. Rev. A **37**, 3313 (1988), and references included.
[8] A. Oppenländer, E. Justiniano, R. Schuch, M. Schulz, W. Schadt, H. Schmidt-Böcking, and P. Roke, GSI-Annual Report 1985 (unpublished), p. 183.
[9] G. Wintermeyers, V. Dangendorf, H. Schmidt-Böcking, T. Kambara, P. H. Rokles, R. Schuch, and I. Tserruya, Z. Phys. D **17**, 145 (1990).
[10] P. Thieberger, J. Barette, B. M. Johnson, K. W. Jones, M. Meron, and H. E. Wegner, IEEE Trans. Nucl. Sci. **30**, 1431 (1983).
[11] C. L. Cocke, P. Richard, J. S. Eck, and R. Pardo, Nucl. Instrum. Methods B **10**, 838 (1985).
[12] H. Ingwersen, E. Jaeschke, and R. Repnow, Nucl. Instrum. Methods **215**, 55 (1983).
[13] H. P. Mokler, D. H. H. Hoffman, W. A. Schönfeld, D. Maor, W. E. Meyerhof, and Z. Stachura, Nucl. Instrum. Methods **197**, 391 (1982).
[14] C. M. Lyneis, J. Phys. (Paris) Colloq. **50**, C1-689 (1989).
[15] R. Geller, B. Jacquot, and P. Sortais, Nucl. Instrum. Methods A **243**, 244 (1986).
[16] R. Anholt, Z. Phys. A **288**, 257 (1978).
[17] J. S. Briggs, J. H. Macek, and K. Taulbjerg, J. Phys. B **12**, 1457 (1979).
[18] H. Schmidt-Böcking, M. H. Prior, R. Doerner, H. Berg, J. O. K. Pedersen, C. L. Cocke, M. Stockli, and A. S. Schlachter, Phys. Rev. A **37**, 4640 (1988).
[19] R. Herrmann, M. H. Prior, R. Dörner, H. Schmidt-Böcking, C. M. Lyneis, and U. Wille, Phys. Rev. A **46**, 5631 (1992).
[20] U. Wille (private communication); and see J. Eichler and U. Wille, Phys. Rev. A **11**, 1973 (1975).